Triangle singularity in $B^0 \to \pi^- K^+ X(3872)$ via the $D_{s1}\bar{D}D^*$ loop and possible precise measurement of the $X(3872)$ mass

Mao-Jun Yan,[1,2] Ying-Hui Ge,[1] and Xiao-Hai Liu[1,*]

[1]*Center for Joint Quantum Studies and Department of Physics, School of Science, Tianjin University, Tianjin 300350, China*

[2]*CAS Key Laboratory of Theoretical Physics, Institute of Theoretical Physics, Chinese Academy of Sciences, Beijing 100190, China*

(Received 10 August 2022; accepted 17 November 2022; published 1 December 2022)

We investigate the $B^0 \to \pi^- K^+ X(3872)$ decay via the $D_{s1}(2536)\bar{D}D^*$ rescattering diagram. The line shape of the $K^+X(3872)$ distribution curve around $D_{s1}(2536)\bar{D}$ threshold is very sensitive to the $X(3872)$ mass because the triangle singularity (TS) can be generated from the loop. By means of this characteristic, we can determine whether the $X(3872)$ mass is below or above the $D^{*0}\bar{D}^0$ threshold with high precision. The narrowness of $D_{s1}(2536)$ in the loop is one of the key reasons why the TS mechanism of measuring the $X(3872)$ mass may work. The $X(3872)$ width impact on the $K^+X(3872)$ line shape is also crucial in the TS mechanism. If the width is as large as 1 MeV, the proposed method of measuring the $X(3872)$ mass would be ruined.

DOI: 10.1103/PhysRevD.106.114002

I. INTRODUCTION

The threshold cusp and triangle singularity (TS) have been known for many years. They are kinematic singularities of the S matrix and their locations are determined by kinematic variables instead of the interaction strength, which are different from the pole singularities corresponding to hadrons whose origin is dynamical. The square-root branch point of the amplitude at the normal two-body threshold can produce cusp in the energy distribution. The more complicated TS is a logarithmic Landau singularity of the amplitude, which can appear in the physical region due to three on-shell intermediate particles in the loop diagram. Observable effects produced from the threshold cusp and TS, especially the latter, have received more and more attention in recent years. Although some observable effects induced by the TS have been noticed as early as the 1960s, there were limited processes that were accessible in experiments at that time. With the development of experiments, there have been quite a few exotic phenomena that are suggested to result from the TS. We refer to Ref. [1] for a recent review about the threshold cusp and TS in hadronic reactions.

One of the significant high-energy experimental achievements in recent years is the discovery of dozens of exotic hadrons, many of which are also named as XYZ particles (see Refs. [2–11] for a review). An intriguing feature of these exotic states is that many of them are located close to two-hadron thresholds. This is the reason why many of them are regarded as hadronic molecules in numerous papers. Among those candidates of hadronic molecules, the $X(3872)$ [also known as $\chi_{c1}(3872)$ in Ref. [2]] could be the most famous one. It is the first unconventional charmoniumlike state observed in the experiment [12]. Its J^{PC} quantum numbers are determined to be 1^{++} which thus could be the candidate for the quark model state $\chi_{c1}(2P)$. Its preferred decay mode of $\gamma\psi(2S)$ over $\gamma J/\psi$ also favors the $\chi_{c1}(2P)$ assignment. Furthermore, its large production rate at LHC [13–15] and Tevatron [16] implies that it may contain a compact component. However, its mass is just in the vicinity of the $D^{*0}\bar{D}^0$ ($D^0\bar{D}^{*0}$) threshold, which is far from the quark model prediction. The 2022 Particle Data Group (PDG) world-average value is $m_X = 3871.65 \pm 0.06$ MeV [2]. The $D^{*0}\bar{D}^0$ ($D^0\bar{D}^{*0}$) threshold is $m_{D^0} + m_{D^{*0}} = 3871.69 \pm 0.07$ MeV. Then the difference is

$$\delta_X \equiv m_{D^0} + m_{D^{*0}} - m_X = 0.04 \pm 0.09 \text{ MeV}. \quad (1)$$

The incredible closeness of the m_X to the $D^{*0}\bar{D}^0$ ($D^0\bar{D}^{*0}$) threshold together with the large branching ratio of the $X(3872)$ into $D^{*0}\bar{D}^0 + \text{c.c.}$ suggest that the natural explanation of $X(3872)$ could be a hadronic molecule. In this case, the δ_X can be understood as the binding energy. One

*xiaohai.liu@tju.edu.cn

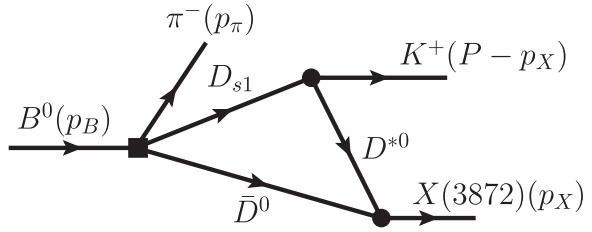

FIG. 1. $B^0 \to \pi^- K^+ X(3872)$ via the $D_{s1}(2536)^+ \bar{D}^0 D^{*0}$ triangle rescattering diagram. We define the invariant $M_{KX}^2 \equiv P^2 \equiv (p_B - p_\pi)^2$.

can find experimental evidence for both the compact state and hadronic molecule interpretations of the $X(3872)$. Although the $X(3872)$ has been well experimentally established by now, its intrinsic structure is still quite puzzling.

From the above δ_X value, one can see the m_X is still indistinguishable from the $D^{*0}\bar{D}^0$ ($D^0\bar{D}^{*0}$) threshold at current levels of precision, i.e., whether the $X(3872)$ mass is above or below $D^{*0}\bar{D}^0$ ($D^0\bar{D}^{*0}$) threshold is still unknown, while a high accuracy mass determination of the $X(3872)$ is very important in understanding its underlying structure. In a recent paper [17] a novel method was proposed to measure the $X(3872)$ mass precisely by measuring the $\gamma X(3872)$ line shape. In the rescattering process $D^{*0}\bar{D}^{*0} \to \gamma X(3872)$, where $D^{*0}\bar{D}^{*0}$ would be produced by a short-distance source, the line shape of the $\gamma X(3872)$ invariant mass spectrum is very sensitive to the m_X or the binding energy δ_X defined above. This is because the TS location of the rescattering diagram is rather sensitive to the particle masses involved. For $\delta_X > 0$ and $\delta_X \leq 0$, the corresponding line shapes show a significant discrepancy.

In Refs. [17,18], the $D^{*0}\bar{D}^{*0}$ pair produced from the short-distance source is set to be in the S wave. In Refs. [19,20], the authors implement this TS mechanism and give a possible reaction $e^+e^- \to \gamma X(3872)$ via the $D^{*0}\bar{D}^{*0}$ rescattering in the P wave. Although the P-wave scattering may smooth the TS peak to some extent, this kind of measurement may be available at current electron-positron colliders. Another similar method, which measures the $\pi X(3872)$ invariant mass spectrum in the $B \to \pi K X(3872)$ process, is also suggested in Refs. [21,22]. Besides, the production of the double-charm tetraquark candidate $T_{cc}^+(3875)$ via a similar D^*D^*D triangle rescattering diagram was also studied in Ref. [23].

The TSs in the above studies concerning the $X(3872)$ production are all developed from the $D^*\bar{D}^*D$ triangle loops, where $D^*\bar{D}^*$ scatter into $\gamma X(3872)$ or $\pi X(3872)$ via exchanging the D meson. One important reason why this novel method of measuring the $X(3872)$ mass may work is that the D^* ($\bar{D}^*$) meson in the triangle diagram is quite narrow, which leads to the line shape of the $\gamma X(3872)$ or $\pi X(3872)$ spectrum being sensitive to the mass of $X(3872)$. Besides the $D^*\bar{D}^*D$ triangle loops, a similar scenario may also appear in other processes. In this work, we suggest measuring the $KX(3872)$ distribution in $B \to \pi K X(3872)$ via the $D_{s1}\bar{D}D^*$ loop, which possesses some special advantages for the determination of m_X.

II. THE MODEL

A. TS mechanism

The $B^0 \to \pi^- K^+ X(3872)$ is one of the reactions where the $X(3872)$ is discovered, of which the branching fraction is around $(2.1 \pm 0.8) \times 10^{-4}$ [24,25]. We notice that this process may receive contributions from the triangle diagram displayed in Fig. 1. In this rescattering process, the $B^0 \to \pi^- D_{s1}(2536)\bar{D}^0$ is a Cabibbo-favored decay, and the $D_{s1}(2536)$ mainly decays into D^*K. Therefore we can expect this rescattering may play a role in $B^0 \to \pi^- K^+ X(3872)$. Furthermore, the intriguing feature of this rescattering process is that the three intermediate particles can be (nearly) on shell simultaneously in some kinematic regions, and a TS located close to the physical boundary in the complex energy plane of the amplitude can develop from this $D_{s1}\bar{D}D^*$ loop. As a result, the transition amplitude of $B^0 \to \pi^- K^+ X(3872)$ will be enhanced in some areas and a TS peak can be expected to arise in the $K^+X(3872)$ invariant mass spectrum.

Assuming the $X(3872)$ mass m_X is not fixed, the location of the TS in the m_X or M_{KX} complex plane can be determined by solving the Landau equation [26,27]. In terms of Eqs. (3) and (4) of Ref. [28], derived from the Landau equation and a dispersion analysis, we can obtain the TS window corresponding to Fig. 1:

$$m_X \in [3871.69, 3875.24]\ \text{MeV}, \tag{2}$$

$$M_{KX} \in [4399.93, 4403.66]\ \text{MeV}, \tag{3}$$

where the central mass values of relevant mesons from Ref. [2] are adopted. The meaning of the above window is as follows: When m_X increases from 3871.69 MeV, i.e., the $D^{*0}\bar{D}^0$ threshold, to 3875.24 MeV, the TS in M_{KX} moves from 4403.66 to 4399.93 MeV; vice versa, when M_{KX} increase from 4399.93 MeV, i.e., the $D_{s1}(2536)\bar{D}^0$ threshold, to 4403.66 MeV, the TS in m_X moves from 3875.24 to 3871.69 MeV. We also refer to Refs. [26–30] for a more detailed discussion on the locations of the TS in various kinematic configurations.

For the $D^*\bar{D}^*D$ loop mentioned in the Introduction, ignoring the D^* width, when $\delta_X = 0$, the TS position of $M_{\gamma X}$ is about 2.7 MeV larger than the $D^*\bar{D}^*$ threshold, while that of $M_{\pi X}$ is 0.3 MeV. For the $D_{s1}\bar{D}D^*$ loop, ignoring the $D_{s1}(2536)$ width, when $\delta_X = 0$, the TS position of M_{KX} is 3.7 MeV larger than the $D_{s1}\bar{D}^0$ threshold. The larger gap between the TS position and pertinent threshold indicates that the line shape could be more sensitive to the $X(3872)$ mass compared with the

$D^* \bar{D}^* D$ loop. Besides, the charm-strange meson $D_{s1}(2536)$ is also very narrow. The PDG average value is $\Gamma(D_{s1}(2536)^{\pm}) = 0.92 \pm 0.05$ MeV [2]. The narrowness of intermediate particles in the triangle diagram is one of the key reasons why the TS mechanism of measuring the $X(3872)$ mass may work.

B. Amplitude of $B^0 \to \pi^- K^+ X(3872)$

When employing the TS mechanism to determine the $X(3872)$ mass, we are interested in the line shape of M_{KX} distributions in the vicinity of the $D_{s1}(2536)\bar{D}^0$ threshold; therefore, we only take into account the amplitude involving the lowest angular momentum between $D_{s1}(2536)$ and $\bar{D}^0$. The nonrelativistic amplitude of $B^0 \to \pi^- D_{s1}\bar{D}^0$ reads

$$t_{B^0 \to \pi^- D_{s1}\bar{D}^0} = \mathcal{C}_1 \vec{\epsilon}^*(D_{s1}) \cdot \vec{p}_\pi, \tag{4}$$

with $\vec{P} = -\vec{p}_\pi + \vec{p}_B = 0$ in the $D_{s1}(2536)\bar{D}^0$ c.m. frame. The coupling constant $\mathcal{C}_1$ can be determined from the experimental data. However, the branching fraction of $B^0 \to \pi^- D_{s1}(2536)\bar{D}^0$ is not known yet. The experiments give $\mathcal{B}(B^0 \to D_{s1}(2536)^+ D^{*-}) \times \mathcal{B}(D_{s1}(2536)^+ \to (D^{*0}K^+ + D^{*+}K^0)) = (5.0 \pm 1.4) \times 10^{-4}$ and $\mathcal{B}(D^{*-} \to \pi^- \bar{D}^0) = (67.7 \pm 0.5)\%$ [2]. Assuming the $\pi^- \bar{D}^0$ states in $B^0 \to \pi^- D_{s1}(2536)\bar{D}^0$ are fully from the $D^{*-} \to \pi^- \bar{D}^0$ decays, we estimate the coupling constant $\mathcal{C}_1 \approx 7.0 \times 10^{-6}$ GeV^{-1} using the experimental central values.

The $D_{s1}(2536)$ mainly decays into D^*K in the relative S wave, and the amplitude for $D_{s1}(2536)^+ \to D^{*0}K^+$ reads

$$t_{D_{s1} \to D^{*0}K^+} = g_{D_{s1}D^*K} \vec{\epsilon}(D_{s1}) \cdot \vec{\epsilon}^*(D^{*0}). \tag{5}$$

To estimate the coupling constant $g_{D_{s1}D^*K}$, we assume that the total decay width of $D_{s1}(2536)^+$ is saturated by the $D^{*0}K^+$ and $D^{*+}K^0$ channels, which share the same coupling constant $g_{D_{s1}D^*K}$ by taking into account the isospin symmetry. The Belle Collaboration studied the angular distributions in the $D_{s1}(2536) \to D^*K$ decays and reported the S-wave partial width $\Gamma_S/\Gamma_{\text{total}} = 0.72 \pm 0.05 \pm 0.01$ [31]. Using the central values of the experimental results, we obtain $g_{D_{s1}D^*K} \approx 0.58$ GeV. Actually, this S-wave decay mode is supposed to be suppressed by the heavy quark spin symmetry. On the other hand, the heavy quark spin symmetry is preserved for the D^*K D-wave decay mode, but this mode is highly suppressed by the limited phase space, since the D^*K threshold is rather close to the $D_{s1}(2536)$ mass. These reasons indicate that the $D_{s1}(2536)$ is so narrow, and we can take advantage of this characteristic to make the TS mechanism work. For another charmed-strange meson $D_{s2}(2573)$, which can also decay into D^*K and whose mass is just a little larger than that of $D_{s1}(2536)$, its width is about 16.9 MeV, which is much larger than $\Gamma_{D_{s1}(2536)}$. We therefore do not take into account the contribution from the $D_{s2}\bar{D}D^*$ loop in this work.

For the fusion of $\bar{D}^0$ and D^{*0} into the $X(3872)$, the amplitude can be written as

$$t_{XD^0\bar{D}^{*0}} = \frac{g_X}{2} \vec{\epsilon}(\bar{D}^{*0}) \cdot \vec{\epsilon}^*(X). \tag{6}$$

Supposing the $X(3872)$ is a pure hadronic molecule, the coupling g_X can be estimated by using the Weinberg compositeness condition [32–34], which gives

$$g_X^2 = \frac{16\pi m_X^2}{\mu} \sqrt{2\mu\delta_X}, \tag{7}$$

where δ_X is the binding energy, and μ is the reduced mass of the $\bar{D}^0$ and D^{*0}, i.e., $\mu = m_{\bar{D}^0} m_{D^{*0}}/(m_{\bar{D}^0} + m_{D^{*0}})$. The above equation is valid for the bound state ($\delta_X > 0$). For the resonant case, the coupling can be evaluated as the residue of the $\bar{D}D^*$ scattering T matrix [35]. The coupling g_X only affects the strength of the rescattering amplitude but will not change the line shape of the distribution curve. We therefore take a moderate value $g_X = 3$ GeV which corresponds to the δ_X is at the order of magnitude of 100 keV, as did in Ref. [22]. We should also mention that, although the g_X does not affect the line shape behavior, it intrinsically depends on the nature of $X(3872)$.

The decay amplitude of $B^0 \to \pi^- K^+ X(3872)$ via the $D_{s1}\bar{D}D^*$ triangle loop figured in Fig. 1 reads

$$\mathcal{M} = i \int \frac{d^4q}{(2\pi)^4} \left(\frac{g_X}{2} g_{D_{s1}D^*K} \mathcal{C}_1\right) (\vec{p}_\pi \cdot \vec{\epsilon}^*(X)) \times \frac{1}{((P-q)^2 - m_{D_{s1}}^2)(q^2 - m_{\bar{D}}^2)((p_X - q)^2 - m_{D^*}^2)}. \tag{8}$$

For the spin-1 state, the sum over polarization takes the form $\sum \epsilon_i \epsilon_j^* = \delta_{ij}$. It should be mentioned that we adopt the nonrelativistic amplitudes in Eqs. (4)–(6), but we do not take the nonrelativistic approximations for the denominators of the three propagators in the loop integral as shown in Eq. (8), since the formalism of these vertexes does not affect the line shape behavior around the threshold we are interested in. The line shape of the distribution curve mainly depends the loop integral, which is numerically evaluated by employing the program package *LoopTools* [36].

The partial decay width of $B^0 \to \pi^- K^+ X(3872)$ reads

$$\frac{d\Gamma_{B \to \pi K X}}{dM_{KX}} = \frac{p_K \tilde{p}_\pi}{(2\pi)^3 4 m_B^2} |\mathcal{M}|^2, \tag{9}$$

where

$$p_K = \frac{1}{2M_{KX}} \lambda^{1/2}(M_{KX}^2, m_K^2, m_X^2), \tag{10}$$

$$\tilde{p}_\pi = \frac{1}{2m_B}\lambda^{1/2}(m_B^2, m_\pi^2, M_{KX}^2), \tag{11}$$

with $\lambda(x,y,z) = x^2 + y^2 + z^2 - 2xy - 2yz - 2zx$.

The TS is a logarithmic singularity. To avoid the infinity of the loop integral in the physical region, one can replace the Feynman's $i\epsilon$ for the propagator by $im\Gamma$ with Γ the total decay width, or equivalently replace the real mass m by the complex mass $m - i\Gamma/2$, which will remove the TS from the physical boundary by a small distance [37–39]. The physical meaning of this complex mass prescription for avoiding the infinity is obvious. As long as the kinematic conditions for the TS being present on the physical boundary are fulfilled, it implies that the intermediate state [here $D_{s1}(2536)$] is unstable, and it is necessary to take the finite width effect into account. Correspondingly, we replace the mass $m_{D_{s1}}$ in Eq. (8) by $m_{D_{s1}} - i\Gamma_{D_{s1}}/2$. The central values $m_{D_{s1}} = 2535.11$ MeV and $\Gamma_{D_{s1}} = 0.92$ MeV from Ref. [2] are adopted in the numerical calculations.

The invariant mass distributions of $K^+X(3872)$ via the triangle diagram in Fig. 1 are displayed in Fig. 2. The $X(3872)$ mass is varied in a window $\delta_X \in [-150, 150]$ keV. One can see that for different m_X or δ_X, the line shapes are also quite different. For every distribution curve in Fig. 2, there is a cusp just at the $D_{s1}(2536)\bar{D}^0$ threshold. But these threshold cusps are smeared to some extent by the width effect of $D_{s1}(2536)$. The peak looks more clear and narrower for the negative δ_X compared with that for the positive δ_X. Supposing the masses of intermediate states are real, if m_X is larger than or equal to the $D^{*0}\bar{D}^0$ threshold ($\delta_X \leq 0$), the TS in M_{KX} can be present on the physical boundary, and the corresponding TS peak in the distribution curve can be very sharp and the peak position is a little bit higher than the $D_{s1}(2536)\bar{D}^0$ threshold, but if m_X is smaller than the $D^{*0}\bar{D}^0$ threshold ($\delta_X > 0$), the conditions of TS in M_{KX} being present on the physical boundary can never be fulfilled, and one does not expect a sharp peak to appear in the distribution curve. Just because of this special character, the line shapes of M_{KX} spectrum are very sensitive to the m_X. Especially, one can easily distinguish whether the δ_X is positive or negative by measuring the $K^+X(3872)$ spectrum.

For the peaks shown in Fig. 2, if we define a "width" at half maximum of the line shape, we can see the width can be as large as 3 to 5 MeV. Although this width is not a well-defined quantity because of the asymmetric line shape, we can still see an advantage for experiment: the larger width of the TS peak may reduce the requirement for the energy resolution in measuring the line shape. The larger width is related to the larger TS window as shown in Eq. (3).

Besides the $D_{s1}(2536)^+\bar{D}^0D^{*0}$ rescattering diagram shown in Fig. 1, the $B^0 \to \pi^- K^+ X(3872)$ process may receive other contributions, such as the cascade decay process $B^0 \to K^{*0}X(3872) \to \pi^- K^+ X(3872)$. The experiment gives the branching fraction $\mathcal{B}(B^0 \to K^{*0}X(3872)) = (1.0 \pm 0.5) \times 10^{-4}$ [2]; we then have $\mathcal{B}(B^0 \to K^{*0}X(3872)) \times B(K^{*0} \to \pi^- K^+) \approx 0.67 \times 10^{-4}$. One may notice that the contribution of this cascade decay process is sizeable and much larger than that of the $D_{s1}(2536)^+\bar{D}^0D^{*0}$ rescattering diagram. However, in the $K^+X(3872)$ invariant mass spectrum, especially around the vicinity of $D_{s1}(2536)\bar{D}^0$ threshold we are interested in, the contribution of the cascade process to $B^0 \to \pi^- K^+ X(3872)$ only serves as a smooth background. The $D^*\bar{D}^*D$ triangle rescattering diagram as studied in Refs. [21,22] can also contribute to the $B^0 \to \pi^- K^+ X(3872)$ decay. Using the similar model and the same coupling constants adopted in Ref. [22], we estimate the contribution of the $D^*\bar{D}^*D$ rescattering diagram to the $K^+X(3872)$ spectrum. The numerical results are shown in Fig. 3. One may notice that the contribution of the $D^*\bar{D}^*D$ diagram is relatively larger than that of the $D_{s1}(2536)^+\bar{D}^0D^{*0}$ diagram. However, the distribution is very flat around the $D_{s1}(2536)\bar{D}^0$ threshold. For the $D^*\bar{D}^*D$

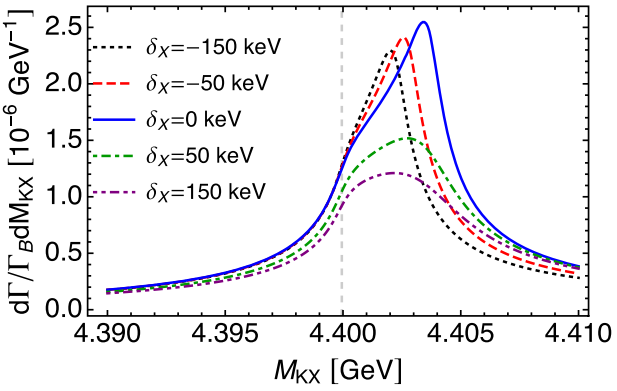

FIG. 2. The $K^+X(3872)$ invariant mass distributions around the $D_{s1}(2536)\bar{D}^0$ threshold (vertical dashed line) via the rescattering process in Fig. 1. Different curves correspond to different $X(3872)$ masses.

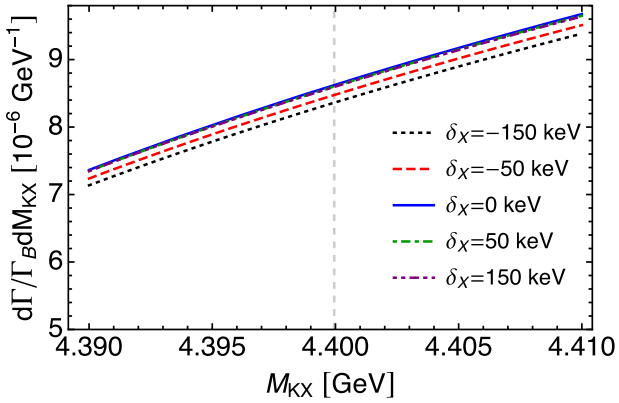

FIG. 3. The $K^+X(3872)$ invariant mass distributions around the $D_{s1}(2536)\bar{D}^0$ threshold (vertical dashed line) via the $D^*\bar{D}^*D$ triangle rescattering diagram. Different curves correspond to different $X(3872)$ masses.

diagram, although in the $\pi^- X(3872)$ spectrum, the TS peak around $D^* \bar{D}^*$ threshold may arise as illustrated in Ref. [22]; in the $K^+ X(3872)$ spectrum this rescattering contribution also only serves as a relatively smooth background. The interference between the $D_{s1}(2536)^+ \bar{D}^0 D^{*0}$ rescattering diagram and the above backgrounds is therefore not included in the current analysis.

C. Width impact of the $X(3872)$

The $X(3872)$ is not a stable particle, and we need to take into account its width impact on the $KX(3872)$ line shape we are interested in. The Belle Collaboration reports the branching fraction $\mathcal{B}(X(3872) \to D^0 \bar{D}^{*0})$ is about 37% [40], and the $\mathcal{B}(X(3872) \to D^0 \bar{D}^0 \pi^0)$ is about 40% with large uncertainties [41]. The partial decay width $\Gamma(X(3872) \to D^0 \bar{D}^0 \pi^0)$ is expected to be about 40 keV in Refs. [42–44]. Then the total width of $X(3872)$ can be estimated at around 100 keV. On the other hand, in Ref. [45], the LHCb Collaboration reports the Breit-Wigner (BW) width of $X(3872)$ is $\Gamma_{BW} = 1.39 \pm 0.24 \pm 0.10$ MeV. But considering that the proximity of $X(3872)$ mass to the $D^0 \bar{D}^{*0}$ threshold may distort the line shape from the simple BW form, the LHCb also reports the full width at half maximum (FWHM) of the line shape is $\Gamma_{FWHM} = 0.22^{+0.07+0.11}_{-0.06-0.13}$ MeV by using a Flatté-inspired model [45]. One can see that the width value is subtle and highly depends on the fitting methods for the near threshold state $X(3872)$. The PDG 2022 gives the averaged BW width $\Gamma_X = 1.19 \pm 0.21$ MeV [2]. We take into account the $X(3872)$ width impact on the KX line shape by introducing a new invariant mass distribution function

$$\frac{d\tilde{\Gamma}_{B\to\pi KX}}{dM_{KX}} = \int_{(m_X-2\Gamma_X)^2}^{(m_X+2\Gamma_X)^2} dm^2 \rho_X(m^2) \frac{d\Gamma_{B\to\pi KX}}{dM_{KX}}, \tag{12}$$

where the spectral function ρ_X is defined to be

$$\rho_X = \frac{1}{\mathcal{N}} \left(-\frac{1}{\pi}\right) \mathrm{Im}\left[\frac{1}{m^2 - m_X^2 + i m_X \Gamma_X}\right], \tag{13}$$

with

$$\mathcal{N} = \int_{(m_X-2\Gamma_X)^2}^{(m_X+2\Gamma_X)^2} dm^2 \left(-\frac{1}{\pi}\right) \mathrm{Im}\left[\frac{1}{m^2 - M_X^2 + i M_X \Gamma_X}\right]. \tag{14}$$

The same functions are adopted in Ref. [22]. Another spectral function with Flatté parametrization is adopted in Ref. [18]. The corresponding new distribution curves are displayed in Fig. 4. Compared with Fig. 2, we can see that the strengths are weakened and the curves are smoothed to some extent. When Γ_X is set to be 100 and 220 keV, one can still see relatively larger discrepancy between the curves corresponding to negative and positive δ_X. To see the sensitivity of the line shape on the narrow width, in Fig. 4(b) the error bands are also plotted by assuming the width Γ_X has an uncertainty of around 15%. One may notice that these error bands are relatively narrower. However, when Γ_X is set to be 1.19 MeV, the discrepancy between different curves is tiny and those curves nearly overlap with each other, which implies the sensitiveness of the line shape on δ_X is reduced when Γ_X is larger. From this point of view,

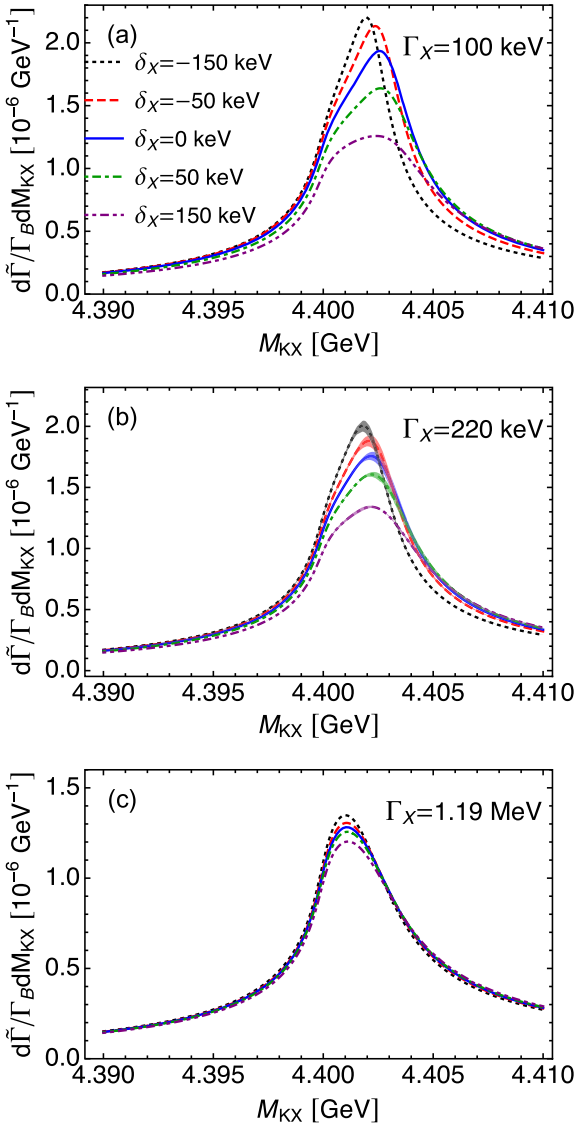

FIG. 4. The $X(3872)$ width dependent $K^+ X(3872)$ invariant mass distributions as defined in Eq. (12) via the rescattering process in Fig. 1. The width of $X(3872)$ is fixed to be (a) 100 keV, (b) 220 keV, and (c) 1.19 MeV, respectively. The dotted, dashed, solid, dot-dashed, and dot-dot-dashed curves corresponds to $\delta_X = -150$, -50, 0, 50 and 150 keV, respectively. The bands in panel (b) are obtained by assuming the width Γ_X has an uncertainty of 15%.

we comment that if the width of $X(3872)$ is as large as 1 MeV, the TS mechanism of measuring its mass may be ruined.

If we use the TS mechanism to measure the discrepancy between m_X and $D^{*0}\bar{D}^0$ threshold, the $X(3872)$ needs to be reconstructed in decay modes other than the $D^0\bar{D}^0\pi^0$, which can be $J/\psi\pi^+\pi^-$, $J/\psi\pi^+\pi^-\pi^0$ and so on. Otherwise one has to take into account the interference term between the rescattering triangle diagram and the cascade decay process $B^0 \to \pi^- D_{s1}(2536)^+\bar{D}^0 \to \pi^- K^+ D^0\bar{D}^0\pi^0$. This interference is subtle and the tree level cascade decay process cannot be treated as a smooth background near the TS regions because of the so-called Schmid theorem [46–50]. This point has even been pointed out in Ref. [17].

III. SUMMARY

In summary, we investigate the $B^0 \to \pi^- K^+ X(3872)$ decay via a triangle rescattering diagram, where the $B^0 \to \pi^- D_{s1}(2536)^+\bar{D}^0$ decay followed by $D_{s1}(2536)^+$ decaying into $D^{*0}K^+$ and $D^{*0}\bar{D}^0$ fusing into $X(3872)$. The TS of the rescattering amplitude can be generated from the $D_{s1}(2536)\bar{D}D^*$ loop, and the line shape of $K^+X(3872)$ distribution curve is very sensitive to the $X(3872)$ mass. By means of this characteristic, we can determine whether the $X(3872)$ mass is below or above the $D^{*0}\bar{D}^0$ threshold, which is crucial in understanding the nature of $X(3872)$. The narrowness of $D_{s1}(2536)$ in this $D_{s1}\bar{D}D^*$ loop is one of the key reasons why the TS mechanism of measuring the $X(3872)$ mass may work. The relatively larger TS kinematic window may also reduce the experimental requirement for energy resolution. This indirect method of measuring the $X(3872)$ mass in the $B^0 \to \pi^- K^+ X(3872)$ decay via the $D_{s1}\bar{D}D^*$ loop may be feasible in the LHCb and updated Belle II experiments.

We also take into account the $X(3872)$ width impact on the KX line shape by introducing a distribution function convoluted with the $X(3872)$ spectral function. It is shown that for the $X(3872)$ width to be at the order of 100 keV, the influence of the width is small. But if the $X(3872)$ width is as large as 1 MeV, the method of using the TS mechanism to precisely measure its mass would be ruined.

ACKNOWLEDGMENTS

This work is supported in part by the National Natural Science Foundation of China (NSFC) under Grants No. 11975165, No. 12235018, No. 11835015, No. 12047503, and No. 12125507; the Chinese Academy of Sciences under Grant No. XDB34030000; and the China Postdoctoral Science Foundation under Grant No. 2022M713229.

[1] F. K. Guo, X. H. Liu, and S. Sakai, Prog. Part. Nucl. Phys. **112**, 103757 (2020).
[2] R. L. Workman *et al.* (Particle Data Group), Prog. Theor. Exp. Phys. **2022**, 083C01 (2022).
[3] F. K. Guo, C. Hanhart, U. G. Meißner, Q. Wang, Q. Zhao, and B. S. Zou, Rev. Mod. Phys. **90**, 015004 (2018); **94**, 029901(E) (2022).
[4] Y. S. Kalashnikova and A. V. Nefediev, Phys. Usp. **62**, 568 (2019).
[5] N. Brambilla, S. Eidelman, C. Hanhart, A. Nefediev, C. P. Shen, C. E. Thomas, A. Vairo, and C. Z. Yuan, Phys. Rep. **873**, 1 (2020).
[6] H. X. Chen, W. Chen, X. Liu, and S. L. Zhu, Phys. Rep. **639**, 1 (2016).
[7] A. Esposito, A. Pilloni, and A. D. Polosa, Phys. Rep. **668**, 1 (2017).
[8] S. L. Olsen, T. Skwarnicki, and D. Zieminska, Rev. Mod. Phys. **90**, 015003 (2018).
[9] R. F. Lebed, R. E. Mitchell, and E. S. Swanson, Prog. Part. Nucl. Phys. **93**, 143 (2017).
[10] A. Ali, J. S. Lange, and S. Stone, Prog. Part. Nucl. Phys. **97**, 123 (2017).
[11] Y. R. Liu, H. X. Chen, W. Chen, X. Liu, and S. L. Zhu, Prog. Part. Nucl. Phys. **107**, 237 (2019).
[12] K. Abe *et al.* (Belle Collaboration), Phys. Rev. Lett. **91**, 262001 (2003).
[13] M. Aaboud *et al.* (ATLAS Collaboration), J. High Energy Phys. 01 (2017) 117.
[14] S. Chatrchyan *et al.* (CMS Collaboration), J. High Energy Phys. 04 (2013) 154.
[15] R. Aaij *et al.* (LHCb Collaboration), Eur. Phys. J. C **72**, 1972 (2012).
[16] V. M. Abazov *et al.* (D0 Collaboration), Phys. Rev. Lett. **93**, 162002 (2004).
[17] F. K. Guo, Phys. Rev. Lett. **122**, 202002 (2019).
[18] S. Sakai, H. J. Jing, and F. K. Guo, Phys. Rev. D **102**, 114041 (2020).
[19] E. Braaten, L. P. He, and K. Ingles, Phys. Rev. D **100**, 031501 (2019).
[20] E. Braaten, L. P. He, and K. Ingles, Phys. Rev. D **101**, 014021 (2020).
[21] E. Braaten, L. P. He, and K. Ingles, Phys. Rev. D **100**, 074028 (2019).
[22] S. Sakai, E. Oset, and F. K. Guo, Phys. Rev. D **101**, 054030 (2020).
[23] E. Braaten, L. P. He, K. Ingles, and J. Jiang, Phys. Rev. D **106**, 034033 (2022).
[24] P. A. Zyla *et al.* (Particle Data Group), Prog. Theor. Exp. Phys. **2020**, 083C01 (2020).
[25] A. Bala *et al.* (Belle Collaboration), Phys. Rev. D **91**, 051101 (2015).
[26] S. Coleman and R. E. Norton, Nuovo Cimento **38**, 438 (1965).

[27] L. D. Landau, Nucl. Phys. **13**, 181 (1959).
[28] X. H. Liu, M. Oka, and Q. Zhao, Phys. Lett. B **753**, 297 (2016).
[29] J. B. Bronzan and C. Kacser, Phys. Rev. **132**, 2703 (1963).
[30] I. J. R. Aitchison, Phys. Rev. **133**, B1257 (1964).
[31] V. Balagura *et al.* (Belle Collaboration), Phys. Rev. D **77**, 032001 (2008).
[32] S. Weinberg, Phys. Rev. **137**, B672 (1965).
[33] V. Baru, J. Haidenbauer, C. Hanhart, Y. Kalashnikova, and A. E. Kudryavtsev, Phys. Lett. B **586**, 53 (2004).
[34] D. Gamermann, J. Nieves, E. Oset, and E. Ruiz Arriola, Phys. Rev. D **81**, 014029 (2010).
[35] D. Gamermann and E. Oset, Phys. Rev. D **80**, 014003 (2009).
[36] T. Hahn, Nucl. Phys. B, Proc. Suppl. **89**, 231 (2000).
[37] I. J. R. Aitchison and C. Kacser, Phys. Rev. **133**, B1239 (1964).
[38] A. Denner and J. N. Lang, Eur. Phys. J. C **75**, 377 (2015).
[39] A. Denner and S. Dittmaier, Nucl. Phys. B, Proc. Suppl. **160**, 22 (2006).
[40] T. Aushev *et al.* (Belle Collaboration), Phys. Rev. D **81**, 031103 (2010).
[41] G. Gokhroo *et al.* (Belle Collaboration), Phys. Rev. Lett. **97**, 162002 (2006).
[42] L. Dai, F. K. Guo, and T. Mehen, Phys. Rev. D **101**, 054024 (2020).
[43] F. K. Guo, C. Hidalgo-Duque, J. Nieves, A. Ozpineci, and M. P. Valderrama, Eur. Phys. J. C **74**, 2885 (2014).
[44] S. Fleming, M. Kusunoki, T. Mehen, and U. van Kolck, Phys. Rev. D **76**, 034006 (2007).
[45] R. Aaij *et al.* (LHCb Collaboration), Phys. Rev. D **102**, 092005 (2020).
[46] C. Schmid, Phys. Rev. **154**, 1363 (1967).
[47] I. J. R. Aitchison and C. Kacser, Phys. Rev. **173**, 1700 (1968).
[48] C. J. Goebel, S. F. Tuan, and W. A. Simmons, Phys. Rev. D **27**, 1069 (1983).
[49] A. V. Anisovich and V. V. Anisovich, Phys. Lett. B **345**, 321 (1995).
[50] V. R. Debastiani, S. Sakai, and E. Oset, Eur. Phys. J. C **79**, 69 (2019).